

POCl₃-based Emitter Diffusion Process with Lower Recombination Current Density and Homogeneous Sheet Resistance for Nanotextured Monocrystalline Silicon with Atmospheric Pressure Dry Etching

N. W. Khan¹, A. I. Ridoy¹, B. Kafle¹, M. Klitzke¹, S. Schmidt¹, L. Clochard², A. Wolf¹, M. Hofmann¹, J. Rentsch¹

¹Fraunhofer Institute for Solar Energy Systems ISE, Heidenhofstr. 2, 79110 Freiburg, Germany

²Nines Photovoltaics, IT Tallaght, Dublin 24, Ireland

Correspondence: ahmed.ismail.ridoy@ise.fraunhofer.de, +49 (0)761 4588 2183

ABSTRACT: In this work, we investigate the emitter sheet resistance and emitter recombination current density by optimizing the POCl₃ emitter diffusion process parameters to achieve improved electrical properties and cell performance. Wafers used in the experiment were boron-doped p-type mono-crystalline silicon samples, nanotextured in an atmospheric pressure dry etching tool (ADE) producing highly textured surfaces and decreased surface reflection. Surface roughness is subsequently reduced by a short isotropic etch, to facilitate the surface passivation. The optimization of the diffusion process is realized by adjusting the phosphorus deposition temperature and its drive-in duration, resulting in decreased emitter saturation current density of ~100 fA/cm² and in more homogeneous emitter sheet resistance of ~105 Ω/sq. Compared to the un-optimized diffusion process, it also leads to a decreased Auger recombination.

Keywords: Atmospheric pressure dry etch (ADE), texturization, nanotexture, diffusion, homojunction.

1 INTRODUCTION

In the photovoltaics industry, wet-chemical etching methods have been used for decades for creating texture on silicon substrates. However, alternative texturing methods are also investigated by the photovoltaic community [1–5].

As an alternative to wet-chemical microtexture, nanotexturing processes have been gaining large interest due to their superior ability for enhanced light entrapment, hence very low surface reflectivity, also referred as black silicon (B-Si) structures [1–5]. One of them is the plasma-less and mask-less atmospheric pressure dry etching (ADE) based on fluorine (F₂) gas capable of texturing monocrystalline silicon wafers [6, 7] as well as multicrystalline silicon wafers [8, 9].

Nanotextured surfaces due to their feature size and enlarged surface area can accumulate large amount of dopant atoms during gas phase emitter diffusion process contributing to increased Auger and surface recombination [10]. Therefore, by optimizing the diffusion process, these losses should be mitigated.

As a continuation in the process development of the ADE technique, for its integration into a solar cell manufacturing process flow, an optimized emitter formation on such a textured surface is beneficial in terms of cell performance. In this work, we present phosphorus oxychloride (POCl₃)-based emitter diffusion process developed for ADE textured p-type monocrystalline silicon (mono-Si) wafers resulting in lowered emitter recombination current density and homogeneous emitter sheet resistance.

2 APPROACH

2.1 Experiment design

The process flow for the wafer precursor preparation is presented in Figure 1(a) while Figure 1(b) presents the process steps followed for the lifetime-test wafer preparation and the characterization techniques involved for different measurements.

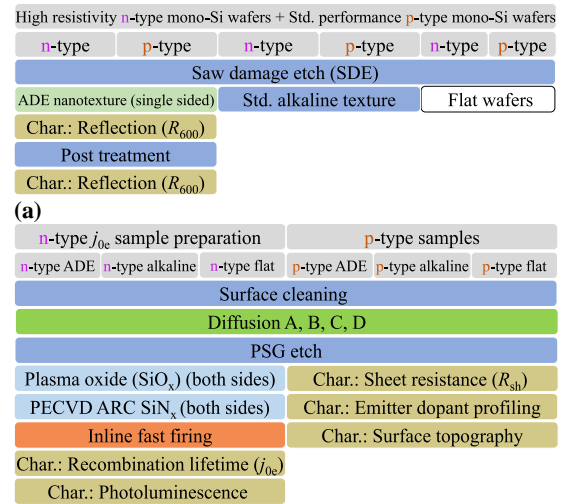


Figure 1: Schematic diagram of process workflows.

Two types of wafers were used in this experiment. Phosphorus-doped n-type wafers with relatively high base resistivity ($5 \Omega\text{cm} \leq \rho_{\text{base}} \leq 7 \Omega\text{cm}$) and boron-doped p-type wafers ($0.8 \Omega\text{cm} \leq \rho_{\text{base}} \leq 1.2 \Omega\text{cm}$). All the wafers (156 mm edge length) were saw-damage etched (SDE) using an alkaline process. One group of the wafers was then processed in the atmospheric pressure dry etching (ADE) tool to produce rough silicon surfaces on one surface of the wafer with reflection at the wavelength of 600 nm (R_{600}) as low as 5% (Figure 2(a)) while the other surface remains saw damage etched (SDE).

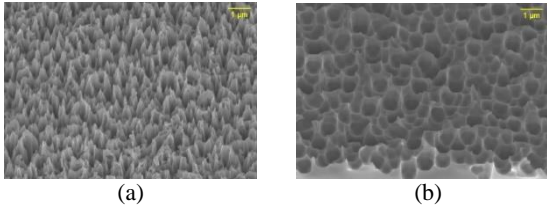


Figure 2: Scanning electron microscopy (SEM) top view images of (a) ADE-textured surface with weighted surface reflection $R_{600} \approx 5\%$, (b) ADE-textured surface after acidic post treatment with weighted surface reflection $R_{600} \approx 10\%$.

Such low reflective surfaces are very challenging to passivate using the standard industrial SiN_x -based plasma-enhanced chemical vapour deposition (PECVD) process [11]. Therefore, the wafers went through an isotropic acidic post-treatment process in order to decrease the surface roughness (Figure 2(b)). Surface reflection of the wafers is measured both before and after the acidic post-treatment. The post-treatment process widens the nanostructures, which on one hand decreases the surface roughness and enables higher surface passivation quality, although on the other hand increases surface reflection.

It is important to note in this experiment that the samples did not have a homogeneous texture across the wafers, as illustrated in Figure 3. Such samples with surface reflection variations from $R_{600} \approx 10\%$ to $R_{600} \approx 18\%$ on a single wafer, present their own challenges for diffusion process optimization as well as PECVD- SiN_x surface passivation [11, 12].

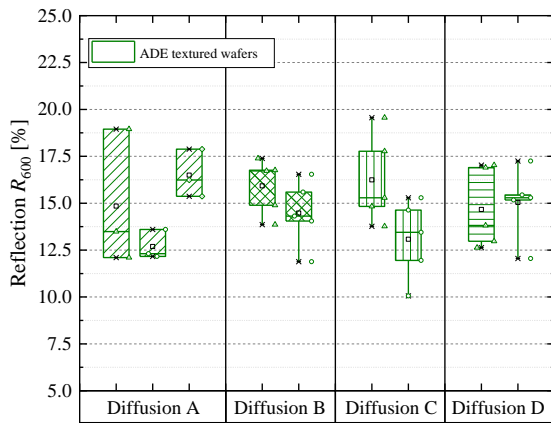


Figure 3: Surface reflection distribution investigating 3 positions on each wafer shown as one block after ADE texture and acidic post treatment. Each diffusion process consists of a group of 2 to 3 wafers.

The second group of wafers is etched in an alkaline solution to produce reference alkaline texture (random pyramids), which is symmetric on both surfaces while the third group is kept as relatively flat reference samples after the SDE process.

The wafers are further divided into two groups in Figure 1(b). All n-type wafers are prepared symmetrically for emitter recombination current density J_{0e} analysis (e.g. ADE process performed on both sides) while the p-type wafers are prepared for other emitter characterization such as emitter dopant profiling and sheet resistance measurements. Four different diffusion

processes (A, B, C, D) were performed in industry-type POCl_3 -based tube diffusion furnace, followed by phosphosilicate glass (PSG) etching.

Table 1 shows the emitter diffusion process parameters which were applied. Two process parameters were varied during these experiments, which were PSG deposition temperature (T_{dep}) and dopant drive-in time ($t_{\text{drive-in}}$). These parameters were varied individually to see their effect on nanotextured surfaces. T_{dep} has major influence on the surface charge carrier concentration and $t_{\text{drive-in}}$ mostly affects the p-n junction depth [13].

Diffusion	Diffusion process parameters	
	PSG deposition Step	Dopant drive-in step
	Temperature (T_{dep}) (°C)	Time ($t_{\text{drive-in}}$) (min.)
A	T	t
B	T-10	t
C	T	2t
D	T-10	2t

Table 1: Emitter diffusion process parameter variations.

Diffusion A was the optimized emitter for standard alkaline texture while diffusion B, C and D were variations of diffusion A, with 10 °C lower deposition temperature and/or a doubled drive in time. The n-type wafers, after PSG etching, are plasma treated to grow a thin plasma oxide followed by PECVD of SiN_x (75 nm on front and rear surfaces as anti-reflection coating (ARC)). After surface passivation, the wafers from all groups were fired at a set temperature of 830°C in a conveyor belt furnace. The p-type wafers were also subjected to the same diffusion variations as the n-type wafers. The PSG was etched after the diffusion process and then the wafers were subjected to emitter characterization.

2.2 Characterization Techniques

N-type wafers from all the diffusion variations were characterized for carrier lifetime using quasi-steady state photoconductance (QSSPC) technique [12]. Lifetime-calibrated photoluminescence (PL) imaging was used to measure spatial carrier lifetime [14]. On the other hand, p-type wafers from all diffusion variations were characterized for emitter sheet resistance (R_{sh}) using four-point probe method (4pp) with 5x5 measurements per wafer [15]. Emitter dopant profile of the p-type wafers was measured using electrochemical capacitance voltage technique (ECV) [15] while the surface topography after ADE texture and acidic post etching was investigated using scanning electron microscopy (SEM) images [15].

3 RESULTS

After the PSG etching, the p-type wafers were subjected to emitter dopant profiling using electrochemical capacitance voltage (ECV) technique. Figure 5 shows these carrier profiles for the ADE nanotextured wafers, standard alkaline textured wafers and reference flat wafers for diffusion A to diffusion D. These profiles are corrected for the emitter sheet resistance locally measured using four-point-probe (4pp) technique.

For the ADE textured wafers in Figure 5(a), diffusion A is the standard process for the alkaline textured wafers.

Diffusion B has lower deposition temperature than diffusion A, which decreases the surface carrier concentration. Otherwise, the carrier concentration profile is very similar to diffusion A. Diffusion C has double dopant drive-in time than diffusion A, which deepens the emitter while also slightly decreases the surface concentration compared to diffusion A as both diffusion A and diffusion C have same T_{dep} .

Diffusion D – having a lower deposition temperature and double drive-in time has lower surface carrier concentration than other variations while the emitter is slightly deeper than diffusions A and B. The emitter depth for diffusion D is lower than diffusion C, despite having the same dopant drive-in time due to lower surface concentration (T_{dep} is lower than diffusion C), which lowers the concentration gradient.

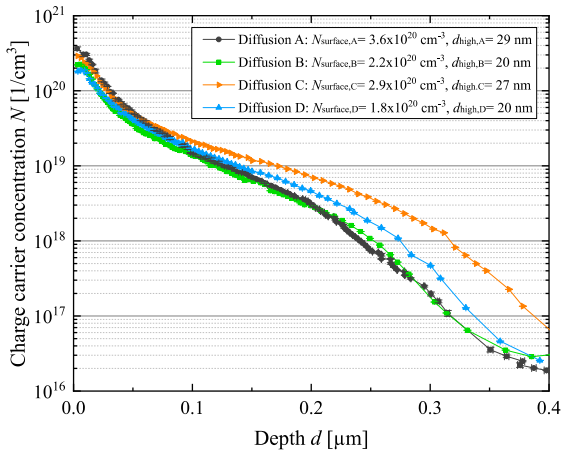


Figure 5(a): Emitter diffusion profile for ADE textured wafers measured by ECV. The profiles are scaled to the locally measured sheet resistance.

Same trend follows for the alkaline textured and flat wafers in Figure 5(b) and Figure 5(c) respectively.

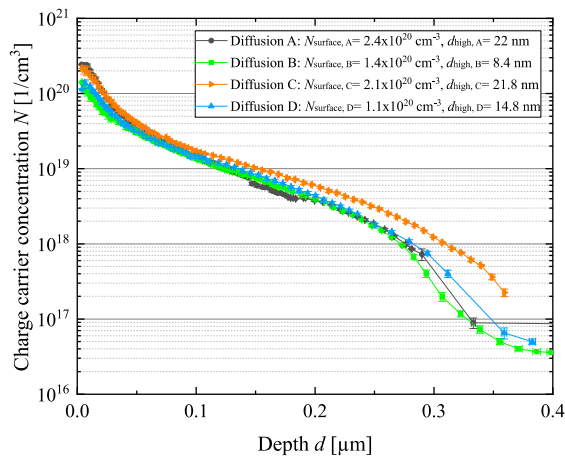


Figure 5(b): Emitter diffusion profile for standard Alkaline textured wafers measured by ECV. The profiles are scaled to the locally measured sheet resistance.

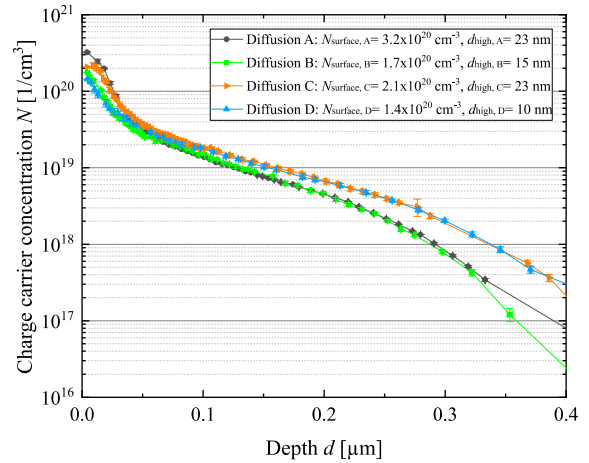


Figure 5(c): Emitter diffusion profile for flat (SDE) wafers measured by ECV. The profiles are scaled to the locally measured sheet resistance.

Figure 6 shows the emitter sheet resistance of ADE textured, alkaline textured and flat wafers measured using 4pp technique. All the wafers in diffusion B show higher sheet resistance compared to all other variations due to lower surface concentration and same emitter depth as diffusion A. The ADE textured wafers in diffusion C have a marginally lower sheet resistance than the standard diffusion A, which is related to deeper emitter (2 times drive-in time). Decreasing T_{dep} from diffusion C to D increases the sheet resistance, in similar fashion for diffusions A and B. The standard deviation in the sheet resistance interprets that diffusion B has slightly higher uniformity than diffusion D for ADE textured wafers. The ADE textured wafers in diffusion C despite having a lower standard deviation in the emitter sheet resistance, could have an increased emitter recombination current density due to lower sheet resistance compared to diffusion A on alkaline texture. Therefore, diffusion B has a better chance of producing an optimized emitter for the ADE textured wafers.

The R_{sh} for ADE-textured wafers, in general, is lower than for alkaline textured wafers for all the diffusion variations, which could be due to the higher surface area of the ADE textured wafers, which accumulates more phosphorus atoms than alkaline-textured wafers.

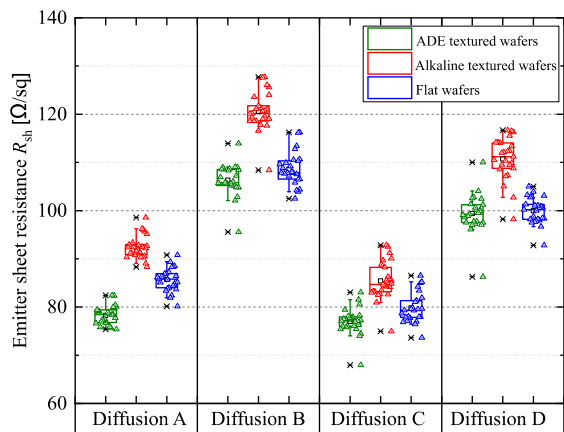


Figure 6: Emitter sheet resistance for ADE-textured, alkaline-textured and flat wafers for diffusion A, B, C and D, measured by 4pp.

Figure 7 shows emitter recombination current density (j_{0e}) of the ADE textured, alkaline textured and flat wafers for different diffusion variations (A, B, C, D). The j_{0e} distribution for the ADE textured wafers follows the reflection distribution shown in Figure 4. Low reflective surfaces tend to have highly textured areas with deeper texture, which could potentially be highly doped. Looking at diffusion C first, the j_{0e} values for all different wafer types are higher than their corresponding wafer types in diffusion variations B and D. While comparing diffusion B and diffusion D, the average j_{0e} is lower for diffusion B. Thus j_{0e} in Figure 7 shows the expected dependence on the R_{sh} shown in Figure 6.

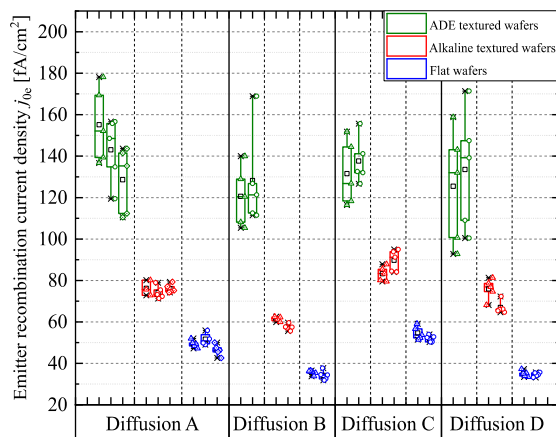


Figure 7: Emitter recombination current density for ADE textured, alkaline textured and flat wafers for diffusion A, B, C and D, measured by QSSPC.

The ADE-textured wafers show that the average j_{0e} for diffusion B is lowest among all the variations. Likewise, alkaline-textured and flat wafers also have lower average j_{0e} for diffusion B, due to the high sheet resistance of this diffusion process. Silicon material is affected by Auger recombination, which depends on charge carrier concentration.

Therefore, wafers in diffusion B having lower carrier concentration while the emitter depth is the same as diffusion A, could potentially have lower Auger recombination. Hence by the optimization of the diffusion process parameters, ADE-textured wafers show better performance in terms of lower emitter recombination current density and higher lifetime.

4 DISCUSSION

The emitter formation by gas phase diffusion using POCl_3 on ADE-textured wafers is certainly different than for alkaline-textured wafers. Nanotextured surfaces due to enlarged surface area potentially accumulate large amounts of phosphorus dopant atoms during POCl_3 diffusion, which leads to higher doping levels and thus increased Auger recombination in the emitter. A diffusion process with lowered PSG deposition temperature yields a lower dose of phosphorus dopants in the emitter, thus decreases the emitter recombination current density j_{0e} by > 12%.

On the other hand, a diffusion process, which applies a higher dopant drive-in time, increased the emitter profile depth but hardly affected the sheet resistance and

the emitter recombination current density for ADE textured surface.

In comparison, the diffusion process having the combination of lower PSG deposition temperature and higher dopant drive-in time shows slight increase in emitter depth and lower surface dopant concentration and higher sheet resistance. For adjusted diffusion parameters, j_{0e} of ADE textured wafers is still higher than the reference alkaline textured wafer, even at similar sheet resistance values.

Therefore, it may be beneficial to further decrease the phosphorus concentration for the ADE-textured wafers by further optimization of the emitter diffusion process parameters.

5 SUMMARY

Nanotextured Si surfaces lead to more pronounced phosphorus diffusion into the Si wafers during POCl_3 -based thermal processes. Lowering the phosphorus amount in the emitter helped to decrease the emitter saturation current density, reaching $\sim 100 \text{ fA/cm}^2$ and a sheet resistance of $\sim 105 \Omega/\text{sq}$.

The most effective method to lower this phosphorus surface concentration was by reducing the PSG deposition temperature.

6 ACKNOWLEDGEMENT

The authors would like to thank KIC InnoEnergy for the financial support of this work within the research project ADE-GLOBAL. The authors would also like to thank all contributing colleagues at the division Photovoltaics of the Fraunhofer ISE who made the development of this work possible. A. I. Ridoy would like to thank the Deutscher Akademischer Austauschdienst (DAAD) for funding the work within the scope of his dissertation.

7 REFERENCES

- [1] K.-s. Lee, M.-H. Ha, J. H. Kim, and J.-W. Jeong, "Damage-free reactive ion etch for high-efficiency large-area multi-crystalline silicon solar cells", *Solar Energy Materials and Solar Cells*, vol. 95, issue 1, p. 66–68, 2011.
- [2] X. X. Lin, Y. Zeng, S. H. Zhong, Z. G. Huang, H. Q. Qian, J. Ling, J. B. Zhu, and W. Z. Shen, "Realization of improved efficiency on nanostructured multicrystalline silicon solar cells for mass production", *Nanotechnology*, vol. 26, issue 12, 125401, 2015.
- [3] J. Rentsch, N. Kohn, F. Bamberg, K. Roth, S. Peters, R. Lüdemann, and R. Preu, "Isotropic plasma texturing of mc-Si for industrial solar cell fabrication", *Proceedings of the 31st IEEE Photovoltaic Specialists Conference*, p. 1316–1319, 2005.
- [4] J. Oh, H.-C. Yuan, and H. M. Branz, "An 18.2%-efficient black-silicon solar cell achieved through control of carrier recombination in nanostructures", *Nature nanotechnology*, vol. 7, issue 11, p. 743–748, 2012.

- [5] B. Kafle, T. Freund, S. Werner, J. Schön, A. Lorenz, A. Wolf, L. Clochard, E. Duffy, P. Saint-Cast, M. Hofmann, and J. Rentsch, "On the nature of emitter diffusion and screen-printing contact formation on nanostructured silicon surfaces", *IEEE J. Photovoltaics*, vol. 7, issue 1, p. 136–143, 2017.
- [6] B. Kafle, T. Freund, A. Mannan, L. Clochard, E. Duffy, S. Werner, P. Saint-Cast, M. Hofmann, J. Rentsch, and R. Preu, "Plasma-free dry-chemical texturing process for high-efficiency multicrystalline silicon solar cells", *Energy Procedia*, vol. 92, p. 359–368, 2016.
- [7] B. Kafle, J. Seiffe, M. Hofmann, L. Clochard, E. Duffy, and J. Rentsch, "Nanostructuring of c-Si surface by F₂-based atmospheric pressure dry texturing process", *Phys. Status Solidi A.*, vol. 212, issue 2, p. 307–311, 2015.
- [8] B. Kafle, A. I. Ridoy, P. Saint-Cast, L. Clochard, E. Duffy, M. Hofmann, and J. Rentsch, "Atmospheric pressure dry texturing enabling > 20% conversion efficiency on multicrystalline silicon PERC solar cells", *AIP Conference Proceedings* 1999, p. 50003 (1–7), 2018.
- [9] P. Saint-Cast, B. Kafle, R. Pandey, A. I. Ridoy, M. Hofmann, L. Clochard, T. Schwarze, M. Pittroff, J. Rentsch, and R. Preu, "Rear passivated mc-Si solar cells textured by atmospheric pressure dry etching", *Energy Procedia*, vol. 124, p. 260–266, 2017.
- [10] B. Kafle, J. Schön, C. Fleischmann, S. Lohmüller (née Werner), A. Wolf, L. Clochard, E. Duffy, M. Hofmann and J. Rentsch, "On the emitter formation in nanotextured silicon solar cells to achieve improved electrical performances", *Solar Energy Materials and Solar Cells*, vol. 152, p. 94–102, 2016
- [11] A. I. Ridoy, B. Kafle, P. Saint-Cast, S. Lohmüller (née Werner), M. H. Norouzi, L. Clochard, E. Duffy, M. Hofmann, J. Rentsch, and R. Preu, "Emitter formation and passivation dependence on crystal grain orientations after atmospheric pressure dry nanotexturing", *35th European Photovoltaic Solar Energy Conference*, Brussels, Belgium, 2018.
- [12] B. Kafle, D. Trogus, B. Dresler, D. Köhler, G. Mäder, L. Clochard, E. Duffy, M. Hofmann, and J. Rentsch, "Industrial screen printed solar cells with novel atmospheric pressure thermochemical dry texturing process", *28th European Photovoltaic Solar Energy Conference*, Paris, France, 2013.
- [13] H. Li, K. Kim, B. Hallam, B. Hoex, S. Wenham and M. Abbott, "POCl₃ diffusion for industrial Si solar cell emitter formation", *Frontiers in Energy*, vol. 11, issue 1, p. 42–51, 2017.
- [14] T. Trupke, B. Mitchell, J. W. Weber, W. McMillan, R. A. Bardos and R. Kroeze, "Photoluminescence imaging for photovoltaic applications", *Energy Procedia*, vol. 15, p. 135–146, 2012.
- [15] D. K. Schroder, "Semiconductor material and device characterization", John Wiley & Sons, 2015